Sensors & Actuators: B. Chemical 381 (2023) 133438

Contents lists available at ScienceDirect

Sensors and Actuators: B. Chemical

journal homepage: www.elsevier.com/locate/snb

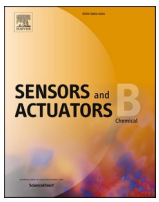

Long-term in-situ real-time fluorescence imaging of lipid droplets during cell ferroptosis process enabled by an epindolidione-based fluorescent probe

Guannan Liu [a], Huanlong Zheng [b], Jianan Dai [a], Huaiyu Li [a], Ri Zhou [a], Chenguang Wang [a,*], Yuan Gao [a], Lijun Wang [a,c], Peng Sun [a,d,**], Fangmeng Liu [a,d], Geyu Lu [a,d]

[a] State Key Laboratory of Integrated Optoelectronics, Key Laboratory of Advanced Gas Sensors of Jilin Province, College of Electronic Science and Engineering, Jilin University, Changchun 130012, China
[b] State Key Laboratory of Supramolecular Structure and Materials, College of Chemistry, Jilin University, Changchun 130012, China
[c] State Key Laboratory of Luminescence and Applications, Changchun Institute of Optics, Fine Mechanics and Physics, Chinese Academy of Sciences, Changchun 130033, China
[d] International Center of Future Science, Jilin University, Changchun 130012, China

ARTICLE INFO

Keywords:
Fluorescence imaging
Fluorescent probes
Photostability
Lipid droplets
Ferroptosis

ABSTRACT

Ferroptosis, as a new form regulation of cell death discovered recently, is triggered by an iron-dependent accumulation of lipid reactive oxygen species and thus closely associated with cellular lipid droplets (LDs). However, directly limited by the un-sufficient photostability and low LDs specificity of common fluorescent probes, visualization of LDs during ferroptosis process particular in a long-term, in-situ, and real-time manner is highly preferred but extremely challenge. To this end, here a new LDs fluorescent probe Lipi-EP featuring with outstanding photostability and high LDs specificity have been rationally developed based on the four-ring-fused epindolidione. Experimentally, the photostability and LDs specificity of this new probe are much higher than the representative LDs probe BODIPY and Nile Red. Consequently, time-lapse multicolor imaging and time-lapse three-dimensional imaging employed this new probe have been successfully conducted to in-situ real-time monitor the LDs change during ferroptosis process up to 6 h. The morphology changes of cellular organelles (LDs, mitochondria and nucleus) and the variations of space distribution of LDs have been impressively visualized. Moreover, the sizes and numbers of LDs have been also determined based on the imaging. This work providing abundant information of LDs would significantly promote the in-depth study of LDs during ferroptosis.

1. Introduction

Cell ferroptosis, newly discovered by Dixon et al. in 2012, is an iron-dependent regulation process of cell death being distinct from the traditional cell apoptosis, necrosis and autophagy [1]. The recent studies demonstrate that cell ferroptosis is driven by inhibiting the lipid repair enzyme glutathione peroxidase 4 (GPX4), which would result in subsequent accumulation of lipid-based reactive oxygen species (ROSs) generated by lipid peroxidation through Fenton reaction [2]. Lipid droplets (LDs), the main cellular organelles storing neutral lipids, are thus necessarily associated with the regulation of ferroptosis. As a result, the study of LDs during ferroptosis process, particular in-situ reveal the change of LDs during such process which would be able to provide abundant and real-time information regarding LDs, is highly important for discovering the new roles and mechanisms of cell ferroptosis [3].

As well known, fluorescence imaging is a powerful method for monitoring subcellular behaviors with the ability of in-situ and real-time detection. So far, a number of LDs fluorescent probes have been developed for LDs imaging and dynamic tracking [4–27]. In particularly, several of them have been used to study the change of LDs during ferroptosis process. For instance, Mao, Liu et al. have developed a polarity-sensitive fluorescent probe CQPP for ratiometric fluorescence imaging and fluorescence lifetime imaging to discover that the LDs polarity would be increased during ferroptosis process [24]. Lin et al. have

* Corresponding author.
** Corresponding author at: State Key Laboratory of Integrated Optoelectronics, Key Laboratory of Advanced Gas Sensors of Jilin Province, College of Electronic Science and Engineering, Jilin University, Changchun 130012, China.
E-mail addresses: wangchenguang@jlu.edu.cn (C. Wang), pengsun@jlu.edu.cn (P. Sun).

https://doi.org/10.1016/j.snb.2023.133438
Received 3 November 2022; Received in revised form 2 January 2023; Accepted 27 January 2023
Available online 27 January 2023

reported a viscosity-sensitive near-infrared (NIR) fluorescent probe BDHT to reveal the increase of LDs viscosity during ferroptosis in an in-situ real-time manner by time-lapse fluorescence imaging [25]. Xiao, Li et al. have represented a fluorescent probe AIE-Cbz-LD-C7 for studying the change of LDs number and the interplay between LDs and endoplasmic reticulum (ER) during ferroptosis [26]. Ye et al. have developed a bifunctional fluorescent probe for LDs imaging and SO2 sensing and have revealed the increase of LDs polarity during ferroptosis [27]. These LDs reports have significantly promoted the study of ferroptosis and provided some new biological insights. Whereas, directly limited by the un-sufficient photostability and/or relatively low LDs specificity, these LDs fluorescent probes are commonly not capable for long-term time-lapse fluorescence imaging. Consequently, monitoring the LDs change during ferroptosis in a long-term, in-situ, and real-time manner is a highly preferred but an extremely challenge task.

In this context, we herein would like to represent a new LDs fluorescent probe Lipi-EP based on the four-ring-fused π-conjugated framework epindolidione. Featuring with the advantages of outstanding photostability and high LDs specificity, this new fluorescent probe has been finely applied in time-lapse multicolor imaging and time-lapse three-dimensional (3D) imaging to in-situ real-time monitor the LDs change during ferroptosis process up to 6 h. As a result, the morphology changes of cellular organelles (LDs, mitochondria and nucleus) and the variations of space distribution of LDs have been impressively demonstrated. Moreover, the sizes and numbers of LDs have been also determined based on the imaging. This work providing abundant information of LDs in multiple perspectives (morphology, space, and metrics) would be thus highly attractive for the biological study of ferroptosis.

2. Experimental section

2.1. Time-lapse multicolor imaging

Live HeLa cells were stained in DMEM+ containing Lipi-EP (2 μM) and 1 % DMSO for 2 h in a CO_2 incubator. Then, the cells were stained in DMEM+ containing MitoTracker Deep Red (50 nM), Hoechst 33342 (20 μM) and 1 % DMSO for 20 min in a CO_2 incubator. After washing with fresh medium, the cells were incubated with DMEM+ containing erastin (10 μM) for imaging. The confocal images were recorded using a Leica TCS SP8 microscope with following set: λ_{exc}: 405 nm, λ_{em}: 415–450 nm for Hoechst 33342; λ_{exc}: 476 nm, λ_{em}: 490–630 nm for Lipi-EP; λ_{exc}: 640 nm, λ_{em}: 650–750 nm for MitoTracker Deep Red.

2.2. Time-lapse 3D imaging

Live HeLa cells were stained in DMEM+ containing Lipi-EP (2 μM) and 1 % DMSO for 2 h in a CO_2 incubator. After washing with fresh medium, the cells were incubated with DMEM+ containing erastin (10 μM) for imaging. The confocal images were recorded using a Leica TCS SP8 microscope with following set: λ_{exc}: 476 nm, λ_{em}: 490–750 nm, a z-step of 200 nm. The reconstruction of 3D confocal image was obtained by the Leica LAS X software.

3. Results and discussion

3.1. Molecular design and synthesis

The design of fluorescent probe Lipi-EP is based on the four-ring-fused π-conjugated framework epindolidione. As an analogue of quinacridone which is a very famous pigment, epindolidione has been synthesized for the first time at 1934 [28]. After that, the study of epindolidione and its derivatives is very limited. Recently, several literatures have revealed that epindolidione derivatives feature with the character of high air stability in the field-effect transistors [29]. These reports inspired us to envision that the photostability of epindolidione may be also very sound. Taken account of further tuning the molecular hydrophobicity and solubility which are critical for selectively labeling cellular LDs [23], the *tert*-butyl groups and propyl chains have been introduced to the epindolidione core, thus providing the target fluorescent probe Lipi-EP.

The synthetic route of Lipi-EP is straight forward (Fig. 1). Starting from dimethyl-2,3-dihydroxyfumarate, the condensation with *tert*-butyl aniline under acid condition readily produced the intermediate **2** which was further undergone Conrad-Limpach reaction to give the semi-cyclized molecule **3**. In next step, it is interesting to found that the Friedel-Crafts reaction of molecule **3** under the nitrogen atmosphere would give the desired molecule **4** while the reaction under the air condition would provide the un-expected molecule **5** (i.e. epindolidione) without the *tert*-butyl moieties. At last, alkylation of molecules **4** and **5** smoothly gave the target fluorescent probe Lipi-EP and its derivative molecule **1**. For the synthetic details and characterization data, please refer to the Supporting Information.

3.2. Photophysical property

The photophysical property of fluorescent probe Lipi-EP has been investigated in various solutions (Fig. 2a and Table S1). Regarding absorptions, this probe displays structured spectra corresponding to various vibration levels ($\nu = 0$, 1, and 2) of excited state. The absorption maxima (λ_{abs}) are around 470 nm with molar absorption coefficients (ε) of about 1.1×10^4 M^{-1} cm^{-1}. In terms of emissions, the probe shows intense green fluorescence with maxima (λ_{em}) and shoulders of around 490 nm and 520 nm, respectively. The absorption and emission spectra featuring with the structured character and the solvent polarity-insensitive behavior demonstrate that the transition of molecule between ground state and excited state is belonged to the π→π * type. Notably, the fluorescence quantum yields (Φ_F) of this probe are good to excellent in various solutions, e.g. 62 % in toluene, 98 % in $CHCl_3$ and 90 % in CH_2Cl_2. In addition, the fluorescence lifetimes (τ) of this probe have been determined to be 8.7–13.0 ns in solutions (Fig. S1). These values are significantly longer than the common organic fluorophores (typically less than 5 ns), revealing the potential application of this probe in fluorescence lifetime imaging [30]. The photophysical property of reference molecule **1** without *tert*-butyl groups has also been investigated (Fig. S2 and Table S1). In overall, the absorption and emission spectra of molecule **1** are similar to those of probe Lipi-EP, while the Φ_F and τ of molecule **1** are obviously lower than the probe.

To deeply understand the transition character of probe Lipi-EP, the time-dependent density functional theory (TD-DFT) calculation has been conducted. As shown in Fig. 2b, both of the highest occupied molecular orbital (HOMO) and the lowest unoccupied molecular orbital (LUMO) are located at the entire four-ring-fused π-conjugated skeleton. The first excited state corresponds to the transition of HOMO to LUMO (an oscillator strength f of 0.0858). Since the HOMO and LUMO are finely overlapped with each other, the π→π * type transition is suggested for probe Lipi-EP, which is consist with the before-mentioned spectral results.

3.3. Fluorescence imaging property

Before imaging experiments, the cytotoxicity of fluorescent probe Lipi-EP and its derivative molecule **1** has been evaluated by 3-(4,5-dimethylthiazol-2-yl)-2,5-diphenyltetrazolium bromide (MTT) assay (Fig. S3). With a concentration up to 10 μM, these two molecules showed negligible cytotoxicity to living cells within 24 h, which indicated the favorable biocompatibility for long-term fluorescence imaging. In next, the co-staining experiments have been conducted to reveal the specificity of this fluorescent probe. The representative mitochondria probe (MitoTracker Deep Red), lysosomes probe (LysoTracker Red), nucleus probe (Hoechst 33342) and LDs probe (Lipi-Red was developed by our group very recently [22]) have been used for these experiments. As shown in Fig. 3, the imaging channel of fluorescent probe Lipi-EP is

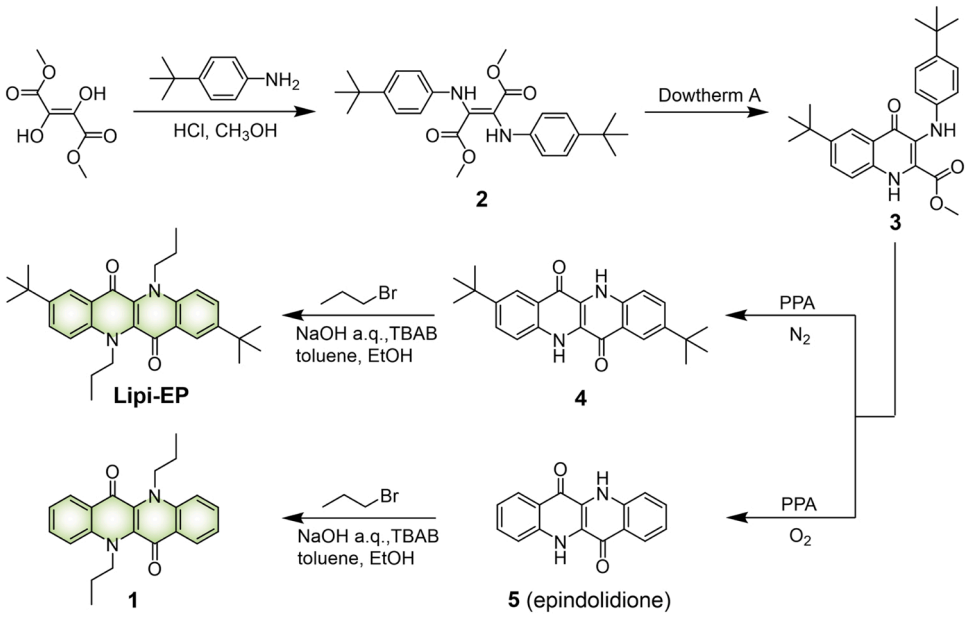

Fig. 1. Synthesis of the fluorescent probe Lipi-EP and its derivative molecule **1**.

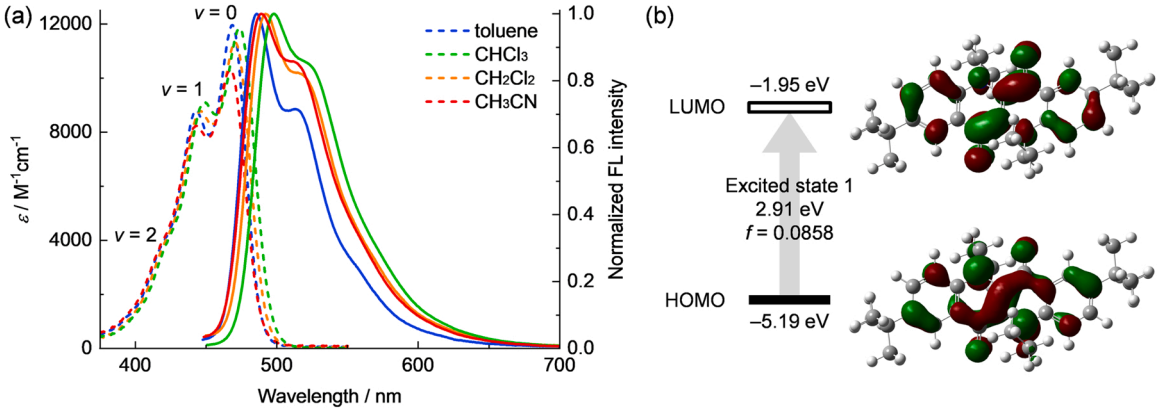

Fig. 2. (a) Absorption and emission spectra of the fluorescent probe Lipi-EP in various solutions. (b) TD-DFT calculation result of the fluorescent probe Lipi-EP.

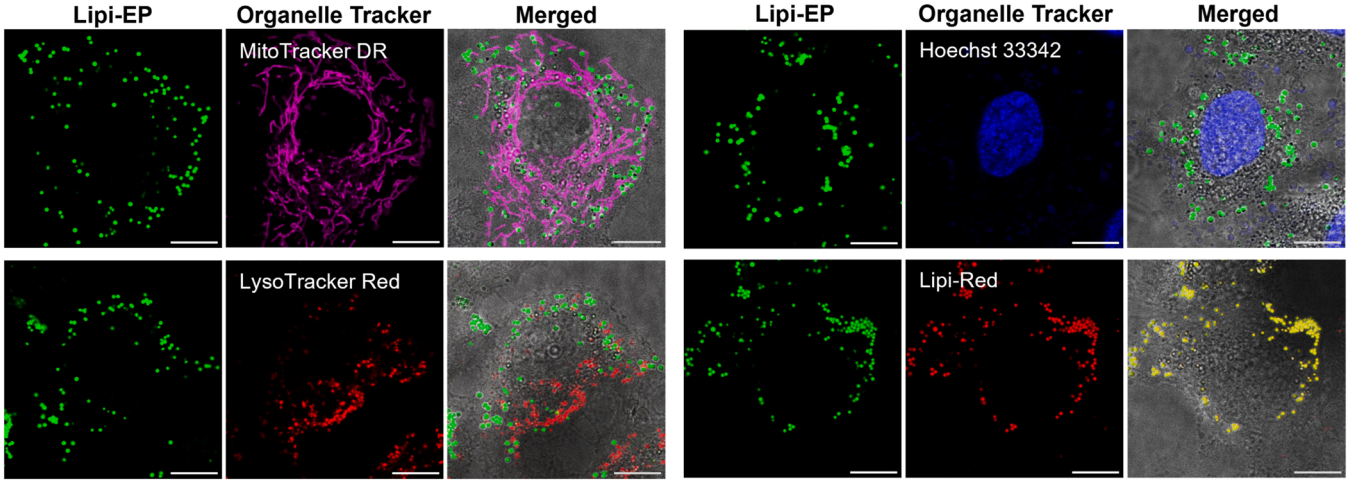

Fig. 3. Co-staining imaging of HeLa cells between the fluorescent probe Lipi-EP and the various organelles trackers (mitochondria, lysosomes, nucleus, and LDs); scale bar: 10 μm.

finely overlapped with that of LDs probe Lipi-Red rather than others. The high Pearson's correlation coefficient value ($R = 0.96$) between the two fluorescent probes confirms the desired LDs specificity of Lipi-EP (Fig. S4).

To further demonstrate its LDs specificity and practical utility, the multicolor confocal imaging which is a very powerful tool to study the interaction between various cellular organelles has been conducted. Taken account of the different emission colors, the green-emissive probe Lipi-EP has been pared with Hoechst 33342 (blue-emissive), LysoTracker Red, MitoTracker Deep Red for the multicolor imaging. As shown in Fig. S5, these fluorescent probes can be selectively imaged in each channel without cross-talk. The merged image of these channels intuitively represents the distributions of cellular nucleus, LDs, lysosomes and mitochondria at the same time. Further employing the multicolor imaging to reveal the change of LDs and mitochondria during ferroptosis process will be illustrated in the following section.

One important advantage of the fluorescent probe Lipi-EP is its high specificity toward LDs. Here, this fluorescent probe has been compared with the most representative LDs probe BODIPY and Nile Red. As shown in Fig. S6, while BODIPY and Nile Red obviously label membrane structure as well besides of LDs, Lipi-EP exclusively stains LDs without any other cellular part. To quantitatively evaluate the LDs specificity of these fluorescent probes, the division values of fluorescence signal intensities between the LDs and their nearby areas are calculated and regarded as the single-to-noise ratios. After 10 times determinations for each fluorescent probe, the single-to-noise ratios have been statistically calculated to be 354 ± 55, 32.9 ± 2.0, and 14.4 ± 0.6 for Lipi-EP, BODIPY, and Nile Red, respectively. Thus, it would be able to state that the LDs specificity of Lipi-EP is ten times higher than BODIPY and twenty times higher than Nile Red. The outstanding LDs specificity is particularly critical for the 3D confocal imaging (vide infra).

The comparison of LDs staining property between fluorescent probe Lipi-EP and its derivative molecule **1** could provide some interesting insights into the molecular structure-property relationship. As shown in Fig. S7, the LDs specificity of molecule **1** is quite poor. This molecule would significantly stain membrane structure as well. Moreover, the fluorescence signal of molecule **1** is much lower than Lipi-EP in cell imaging. Basically, about 10^2 times stronger excitation laser is required for imaging with molecule **1**. Our group has recently pointed out that two factors of fluorescent probe should be considered to largely improve the LDs specificity: 1) a suitable hydrophobicity with CLogP (the calculated *n*-octanol/water partition coefficient) value of around 6 is suggested; 2) a cycloalkyl substituent which has a smaller spatial size than a linear alkyl moiety gives better cell permeability [23]. In the case of this fluorescent probe Lipi-EP, the introduction of two *tert*-butyl groups to molecule **1** suitably increases the CLogP value from 2.3 to 5.9. Moreover, employing the *tert*-butyl group rather than the linear butyl group would provide better cell permeability and thus stronger fluorescence signal for imaging.

Another important advantage of the fluorescent probe Lipi-EP is its high photostability. Under the same intense excitation condition ($\lambda_{ex} =$ 488 nm), the photostability of this probe has been compared with LDs-Red, BODIPY and Nile Red based on continuously recording the confocal images of HeLa cells stained with these fluorescent probes. As shown in Fig. 4a, Lipi-EP is very robust under the harsh imaging condition, while LDs-Red, BODIPY and Nile Red are photobleached very quickly. After recording 300 confocal images, Lipi-EP still maintains 90 % fluorescence intensity relative to its initial value. In contrast, the fluorescence intensities of LDs-Red, BODIPY and Nile Red remain below 40 %, 20 % and 10 %, respectively (Fig. 4b). This comparison highlights the excellent photostability of Lipi-EP which is highly desired for time-lapse fluorescence imaging [31–34]. It also reveals that the epindolidione would be a very attractive fluorophore for constructing new photostable fluorescent probes.

3.4. *In-situ real-time fluorescence imaging of LDs during ferroptosis process*

The advantages of outstanding photostability and high LDs specificity of fluorescent probe Lipi-EP enable to perform time-lapse multicolor imaging as well as time-lapse 3D imaging to in-situ real-time monitor the change of LDs of living cells during ferroptosis process. For the time-lapse multicolor imaging, the HeLa cells pre-stained with Hoechst 33342, Lipi-EP, and MitoTracker Deep Red were imaged with

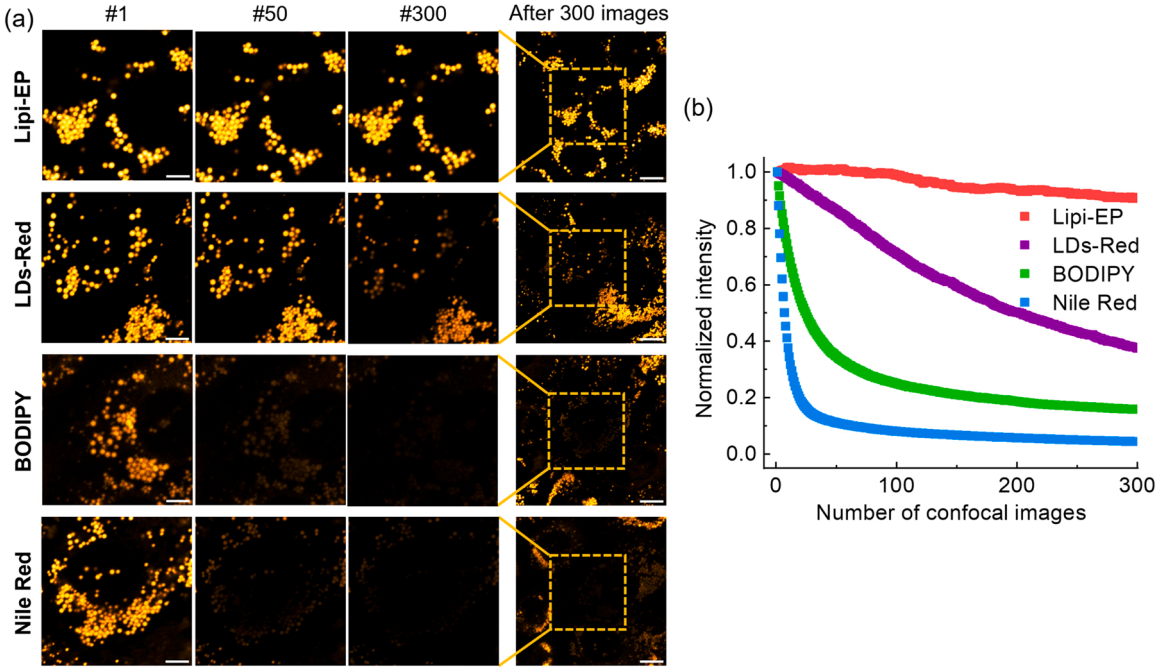

Fig. 4. Comparison of the photostability between Lipi-EP, LDs-Red, BODIPY and Nile Red under the same intense excitation condition. (a) Continuously confocal imaging of HeLa cells stained with these fluorescent probes; the number 1, 50, and 300 images are shown (scale bar: 5 μm); after recoding 300 images, the wider field images are recorded (scale bar: 10 μm). (b) Normalized fluorescence intensity of confocal image plotted as a function of image number.

three channels corresponding to nucleus, LDs, and mitochondria, respectively, as well as one additional channel corresponding to bright field. In a long period of 6 h, 73 multicolor images (i.e. exposure 292 times under the excitation laser) were repeated recorded with a time interval of 5 min. To induce the ferroptosis process, a well-known ferroptosis inducer erastin was added to the culture medium of cells. As shown in Fig. 5 and Movie S1, the cells are in a normal physiological state in the beginning. The morphologies of cells are stretched and the mitochondria have filamentous structures. The LDs and mitochondria are homogeneously dispersed in cells. After that, the cells and their nucleus are gradually contracted under the stimulation of erastin. The mitochondria are also shrunken from filamentous structures to short rod-like morphologies. The LDs and mitochondria are concentrated at around nucleus. After treating with erastin for about 4 h, the cells are died and a crowd of vesicles are appeared surrounding the cells. The fluorescence signals of Hoechst 33342 and MitoTracker Deep Red are lost because these probes would be released out from died cells. During the ferroptosis process, the number of LDs are significantly decreased (precise determination of LDs numbers will be performed by time-lapse 3D imaging in the following section). While the LDs would be not consumed completely, there are still some ones existed in died cells [35]. The size of LDs has been further determined. Their diameters are maintained around 600 nm during the ferroptosis process, without significant change. This result provides an important insight into the biological role of LDs during the ferroptosis process. That is the LDs would be consumed one by one rather than simultaneously consumed all of LDs via deceasing their sizes.

Supplementary material related to this article can be found online at doi:10.1016/j.snb.2023.133438.

Supplementary material related to this article can be found online at doi:10.1016/j.snb.2023.133438.

Time-lapse multicolor imaging has provided the morphology information of cells and organelles during ferroptosis process, and also determined the LDs sizes. Next, time-lapse 3D imaging has been further performed to give the space information of LDs and precisely account the LDs amounts. Generally, a 3D image is reconstructed from dozens of *z*-stack slices. Time-lapse 3D imaging would thus require thousands of imaging scans, which is directly limited by the low photostability of common fluorescent probes. The new fluorescent probe Lipi-EP featured with the excellent photostability is thus highly desired for this purpose. Moreover, the feature of high LDs specificity of Lipi-EP is also critical for clearly visualizing the spatial distribution of LDs in 3D imaging. This viewpoint has been proved by the poor-quality 3D imaging with BODIPY and Nile Red, in which the strong background fluorescence resulted from nonspecific staining significantly covers the LDs (Fig. S8).

For the time-lapse 3D imaging to monitor LDs change during ferroptosis process, 73 acquisitions of 3D images of HeLa cells were conducted in 6 h with a time interval of 5 min. Since one 3D image consisted of 50 *z*-stack slices, this time-lapse 3D imaging required up to 3650 imaging scans. The fluorescent probe Lipi-EP capable of so many imaging scans is really impressive. As show in Fig. 6 and Movie S2, the LDs are homogeneously dispersed in cytoplasm in the beginning. Upon stimulation with erastin, the LDs are gradually aggerated around nucleus due to the contractions of cells. Accordingly, the distribution range of LDs is largely decreased in *xy* plane and significantly increased in *z*-axis. As indicated by the variation range of *z*-depth color, the z-axis range of LDs is around 3 μm at 0 min and obviously increased to about 7 μm at 240 min. The *x*, *y*, and *z* sizes of LDs distribution (about 7–10 μm) are comparable to each other at 240 min, revealing that the LDs distribution is a ball-shaped structure. This result is consistent with the before-mentioned time-lapse multicolor imaging where bright filed ball-shaped morphologies of cells are observed at 240 min. Besides of monitoring the distribution change of LDs in 3D space, time-lapse 3D imaging has been able to precisely study the change of LDs numbers during ferroptosis process. The LDs number is largely decreased from 140 at 0 min to 33 at 360 min in cell 1, and decreased from 102 to 25 in cell 2. To get a statistic result of the change of LDs numbers, another 8 cells have been further studied by a similar time-lapse 3D imaging (Fig. S9 and Movie S3-4). In overall, all of these cells display significantly decrease of LDs numbers. After 360 min, the LDs numbers are decreased to 34 ± 17 % ($n = 10$) of their initial amounts (Fig. S10). Moreover, it is found that the LDs consumption is very fast in the beginning 2–3 h of ferroptosis process and then is slow in the following period. This result highlights the great utility of this superior fluorescent probe for time-lapse 3D imaging, which is very powerful for deeply studying the LDs consumption dynamics and detail process [36].

Supplementary material related to this article can be found online at doi:10.1016/j.snb.2023.133438.

4. Conclusion

In summary, we have rational developed a new LDs fluorescent

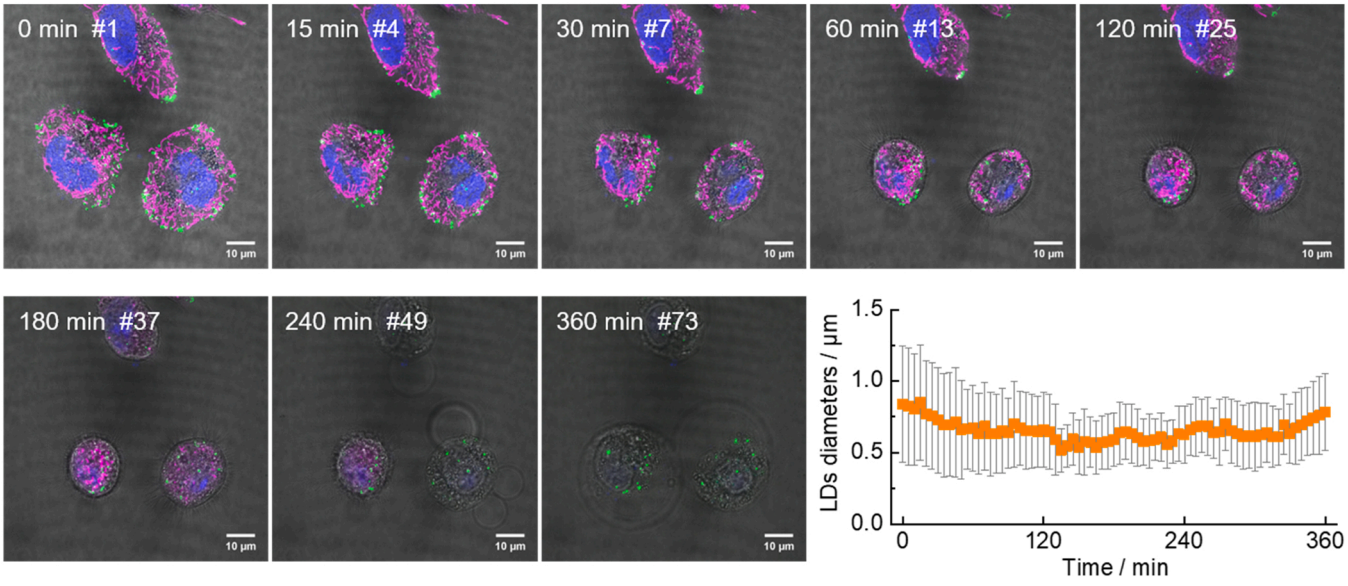

Fig. 5. Time-lapse multicolor imaging to in-situ real-time monitor the change of LDs of living cells during ferroptosis process; scale bar: 10 μm. The HeLa cells were stained with Hoechst 33342, Lipi-EP, and MitoTracker Deep Red. The LDs diameters are determined in the ferroptosis process based on the multicolor imaging.

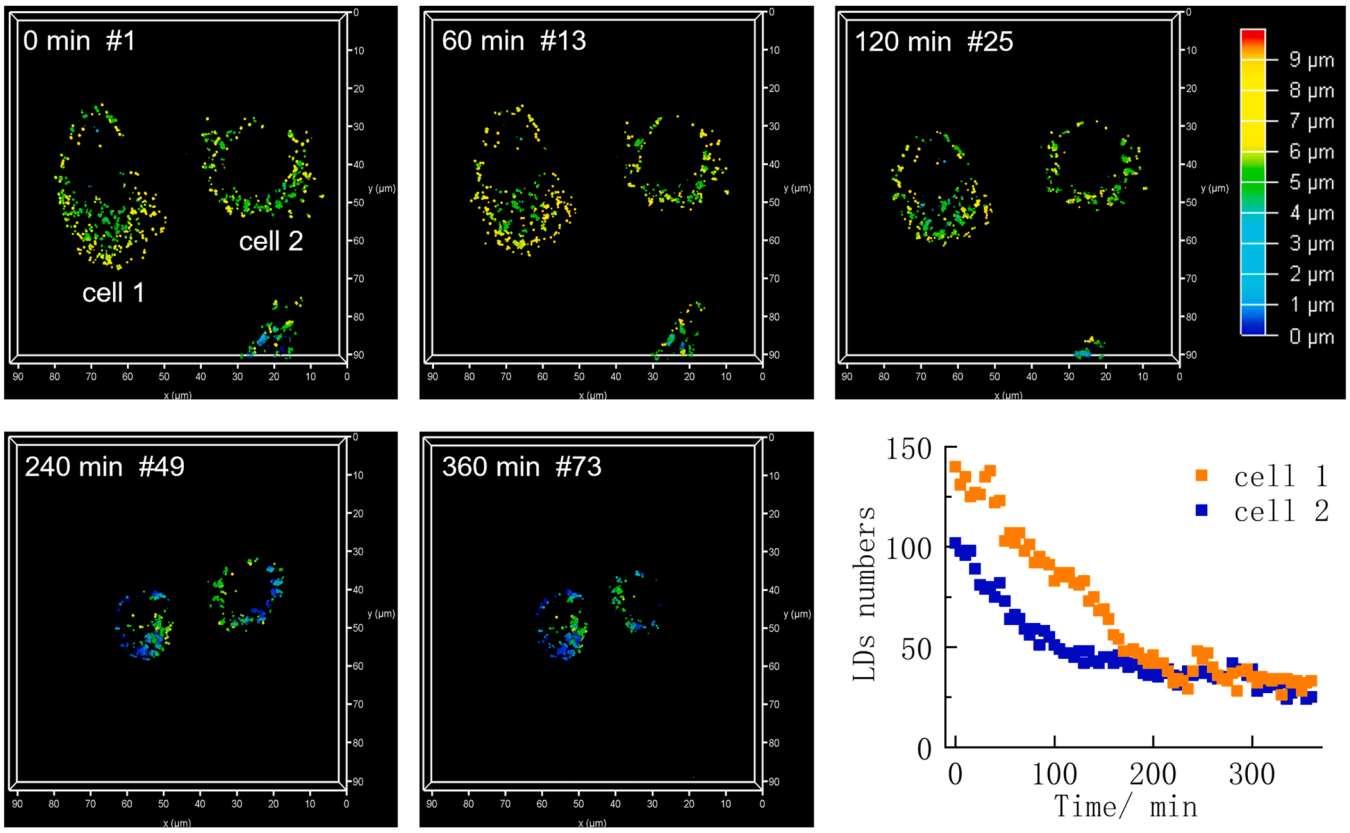

Fig. 6. Time-lapse 3D imaging to in-situ real-time monitor the change of LDs of living HeLa cells during ferroptosis process. The *xyz* imaging size is $92 \times 92 \times 10\ \mu m^3$. The variation of LDs colors means different *z*-depth. The LDs numbers are determined in the ferroptosis process based on the 3D imaging.

probe Lipi-EP based on the old but rarely investigated fluorophore epindolidione. The four-ring-fused rigid structure of epindolidione core endows this fluorescent probe with the feature of outstanding photostability. Finely tuning the alkyl substitutes on the epindolidione core results high LDs specificity which is another feature of this fluorescent probe. The outstanding photostability combined with the high LDs specificity have largely contributed to the visualization of LDs during ferroptosis process in a long-term, in-situ, and real-time manner. For instance, time-lapse multicolor imaging has smoothly conducted to monitor the morphology changes of cellular organelles (LDs, mitochondria and nucleus) and to determine the LDs sizes. Time-lapse 3D imaging has been successfully realized to track the variations of space distribution of LDs and to account the LDs numbers. These fluorescence imaging results providing abundant information regarding LDs in multiple perspectives (morphology, space, and metrics) have helped us to get an important insight into the biological role of LDs during ferroptosis process. We expect that this work would significantly promote the in-depth investigation of LDs during ferroptosis. In addition, it would also inspire the development of new photostable fluorescent probes based on the old epindolidione core.

CRediT authorship contribution statement

Guannan Liu: examined the optical properties, did the cell imaging, wrote the paper. **Huanlong Zheng:** synthesized the fluorescent probe. **Jianan Dai:** analyzed the data. **Huaiyu Li:** analyzed the data. **Ri Zhou:** analyzed the data. **Chenguang Wang:** guided the project, wrote the paper. **Yuan Gao:** guided the project. **Lijun Wang:** guided the project. **Peng Sun:** guided the project, wrote the paper., **Fangmeng Liu:** guided the project. **Geyu Lu:** guided the project.

Declaration of Competing Interest

The authors declare that they have no known competing financial interests or personal relationships that could have appeared to influence the work reported in this paper.

Data Availability

Data will be made available on request.

Acknowledgements

This work is supported by the National Nature Science Foundation of China (61831011, 61833006, 62075079), the China Postdoctoral Science Foundation (2022TQ0112), the Natural Science Foundation of Jilin Province (20220101058JC), the Interdisciplinary Integration and Innovation Project of JLU (JLUXKJC2021QZ08).

Appendix A. Supporting information

Supplementary data associated with this article can be found in the online version at doi:10.1016/j.snb.2023.133438.

References

[1] Scott J. Dixon, Kathryn M. Lemberg, Michael R. Lamprecht, R. Skouta, Eleina M. Zaitsev, Caroline E. Gleason, et al., Ferroptosis: an iron-dependent form of nonapoptotic cell death, Cell 149 (2012) 1060–1072.
[2] B.R. Stockwell, J.P. Friedmann Angeli, H. Bayir, A.I. Bush, M. Conrad, S.J. Dixon, et al., Ferroptosis: a regulated cell death nexus linking metabolism, redox biology, and disease, Cell 171 (2017) 273–285.
[3] J.A. Olzmann, P. Carvalho, Dynamics and functions of lipid droplets, Nat. Rev. Mol. Cell Biol. 20 (2019) 137–155.

[4] R. Zhou, C. Wang, G. Lu, Advances in organic fluorescent probes for super-resolution imaging of cellular lipid droplets, Chin. Opt. 15 (2022) 1228–1242.
[5] M. Collot, T.K. Fam, P. Ashokkumar, O. Faklaris, T. Galli, L. Danglot, et al., Ultrabright and fluorogenic probes for multicolor imaging and tracking of lipid droplets in cells and tissues, J. Am. Chem. Soc. 140 (2018) 5401–5411.
[6] L. Guo, M. Tian, Z. Zhang, Q. Lu, Z. Liu, G. Niu, et al., Simultaneous two-color visualization of lipid droplets and endoplasmic reticulum and their interplay by single fluorescent probes in lambda mode, J. Am. Chem. Soc. 143 (2021) 3169–3179.
[7] J. Chen, C. Wang, W. Liu, Q. Qiao, H. Qi, W. Zhou, et al., Stable super-resolution imaging of lipid droplet dynamics through a buffer strategy with a hydrogen-bond sensitive fluorogenic, Probe Angew. Chem. Int. Ed. 60 (2021) 25104–25113.
[8] M. Taki, K. Kajiwara, E. Yamaguchi, Y. Sato, S. Yamaguchi, Fused thiophene-S,S-dioxide-based super-photostable fluorescent marker for lipid droplets, ACS Mater. Lett. 3 (2021) 42–49.
[9] Y. Yu, H. Xing, H. Park, R. Zhang, C. Peng, H.H.Y. Sung, et al., Deep-red aggregation-induced emission luminogen based on dithiofuvalene-fused benzothiadiazole for lipid droplet-specific imaging, ACS Mater. Lett. 4 (2022) 159–164.
[10] C.-J. Wu, X.-Y. Li, T. Zhu, M. Zhao, Z. Song, S. Li, et al., Exploiting the twisted intramolecular charge transfer effect to construct a wash-free solvatochromic fluorescent lipid droplet probe for fatty liver disease diagnosis, Anal. Chem. 94 (2022) 3881–3887.
[11] F. Meng, J. Niu, H. Zhang, R. Yang, Q. Lu, Y. Yu, et al., Simultaneous visualization of lipid droplets and lysosomes using a single fluorescent probe, Sens. Actuat. B: Chem. 329 (2021), 129148.
[12] M.-X. Liu, N. Ding, S. Chen, Y.-L. Yu, J.-H. Wang, One-step synthesis of carbon nanoparticles capable of long-term tracking lipid droplet for real-time monitoring of lipid catabolism and pharmacodynamic evaluation of lipid-lowering drugs, Anal. Chem. 93 (2021) 5284–5290.
[13] X. Wu, X. Wang, Y. Li, F. Kong, K. Xu, L. Li, et al., A near-infrared probe for specific imaging of lipid droplets in living cells, Anal. Chem. 94 (2022) 4881–4888.
[14] C. Lai, Y. Zhao, X. Zou, Y. Liang, W. Lin, Quantification of lipid droplets polarity for evaluating non-alcoholic fatty liver disease via fluorescence lifetime imaging, Sens. Actuat. B: Chem. 369 (2022), 132267.
[15] C. Liu, J. Yin, B. Lu, W. Lin, Tracking the polarity changes of asthmatic mice by fluorescence imaging, Sens. Actuat. B: Chem. 346 (2021), 130448.
[16] F. Yu, X. Jing, W. Lin, A unique amphipathic polyethylene glycol-based fluorescent probe for the visualization of lipid droplets and discrimination of living and dead cells in biological systems, Sens. Actuat. B: Chem. 302 (2020), 127207.
[17] J. Yin, M. Peng, W. Lin, Two-photon fluorescence imaging of lipid drops polarity toward cancer diagnosis in living cells and tissue, Sens. Actuat. B: Chem. 288 (2019) 251–258.
[18] R. Zhou, C. Wang, X. Liang, F. Liu, P. Sun, X. Yan, X. Jia, X. Liu, Y. Wang, G. Lu, A new organic molecular probe as a powerful tool for fluorescence imaging and biological study of lipid droplets, Theranostics 13 (2023) 95–105.
[19] G. Liu, G. Peng, J. Dai, R. Zhou, C. Wang, X. Yan, et al., STED nanoscopy imaging of cellular lipid droplets employing a superior organic fluorescent probe, Anal. Chem. 93 (2021) 14784–14791.
[20] R. Zhou, C. Wang, X. Liang, F. Liu, X. Yan, X. Liu, et al., Stimulated Emission Depletion (STED) super-resolution imaging with an advanced organic fluorescent probe: visualizing the cellular lipid droplets at the unprecedented nanoscale resolution, ACS Mater. Lett. 3 (2021) 516–524.
[21] G. Liu, J. Dai, R. Zhou, G. Peng, C. Wang, X. Yan, et al., A distyrylbenzene-based fluorescent probe with high photostability and large Stokes shift for STED nanoscopy imaging of cellular lipid droplets, Sens. Actuat. B: Chem. 353 (2022), 131000.
[22] G. Peng, J. Dai, R. Zhou, G. Liu, X. Liu, X. Yan, et al., Highly efficient red/NIR-emissive fluorescent probe with polarity-sensitive character for visualizing cellular lipid droplets and determining their polarity, Anal. Chem. 94 (2022) 12095–12102.
[23] R. Zhou, Y. Cui, J. Dai, C. Wang, X. Liang, X. Yan, et al., A red-emissive fluorescent probe with a compact single-benzene-based skeleton for cell imaging of lipid droplets, Adv. Opt. Mater. 8 (2020) 1902123.
[24] K.-N. Wang, L.-Y. Liu, D. Mao, S. Xu, C.-P. Tan, Q. Cao, et al., A polarity-sensitive ratiometric fluorescence probe for monitoring changes in lipid droplets and nucleus during ferroptosis, Angew. Chem. Int. Ed. 60 (2021) 15095–15100.
[25] B. Dong, W. Song, Y. Lu, Y. Sun, W. Lin, Revealing the viscosity changes in lipid droplets during ferroptosis by the real-time and in situ near-infrared imaging, ACS Sens. 6 (2021) 22–26.
[26] R. Chen, Z. Li, C. Peng, L. Wen, L. Xiao, Y. Li, Rational design of novel lipophilic aggregation-induced emission probes for revealing the dynamics of lipid droplets during lipophagy and ferroptosis, Anal. Chem. 94 (2022) 13432–13439.
[27] P. Xie, J. Liu, X. Yang, W. Zhu, Y. Ye, A bifunctional fluorescent probe for imaging lipid droplets polarity/SO2 during ferroptosis, Sens. Actuat. B: Chem. 365 (2022), 131937.
[28] A.D. Ainley, R. Robinson, The epindoline group part I trial of various methods for the synthesis of epindolidiones, J. Chem. Soc. (1934) 1508–1520.
[29] E.D. Głowacki, M. Irimia-Vladu, M. Kaltenbrunner, J. Gąsiorowski, M.S. White, U. Monkowius, G. Romanazzi, G.P. Suranna, P. Mastrorilli, T. Sekitani, S. Bauer, T. Someya, L. Torsi, N.S. Sariciftci, Hydrogen-bonded semiconducting pigments for air-stable field-effect transistors, Adv. Mater. 25 (2013) 1563–1569.
[30] K.Y. Zhang, Q. Yu, H. Wei, S. Liu, Q. Zhao, W. Huang, Long-lived emissive probes for time-resolved photoluminescence bioimaging and biosensing, Chem. Rev. 118 (2018) 1770–1839.
[31] C. Wang, M. Taki, Y. Sato, A. Fukazawa, T. Higashiyama, S. Yamaguchi, Super-photostable phosphole-based dye for multiple-acquisition stimulated emission depletion imaging, J. Am. Chem. Soc. 139 (2017) 10374–10381.
[32] C. Wang, M. Taki, Y. Sato, Y. Tamura, H. Yaginuma, Y. Okada, S. Yamaguchi, A photostable fluorescent marker for the super-resolution live imaging of the dynamic structure of the mitochondrial cristae, Proc. Natl. Acad. Sci. U. S. A. 116 (2019) 15817–15822.
[33] C. Wang, M. Taki, K. Kajiwara, J. Wang, S. Yamaguchi, Phosphole-oxide-based fluorescent probe for super-resolution stimulated emission depletion live imaging of the lysosome membrane, ACS Mater. Lett. 2 (2020) 705–711.
[34] P. Zhang, X. Guo, J. Gao, H. Liu, C. Wan, J. Li, et al., A Dual-control strategy by phosphate ions and local microviscosity for tracking adenosine triphosphate metabolism in mitochondria and cellular activity dynamically, ACS Sens. 6 (2021) 4225–4233.
[35] L. Magtanong, P.-J. Ko, M. To, J.Y. Cao, G.C. Forcina, A. Tarangelo, et al., Exogenous monounsaturated fatty acids promote a ferroptosis-resistant cell state, Cell Chem. Biol. 26 (2019) 420–432.
[36] X. Chen, C. Yu, R. Kang, G. Kroemer, D. Tang, Cellular degradation systems in ferroptosis, Cell Death Differ. 28 (2021) 1135–1148.

Guannan Liu received his PhD degree from Jilin University of China in 2021. He is now a postdoctoral fellow at Electronics Science and Engineering Department, Jilin University. His current researches focus on the organic fluorescent molecules for bio-imaging.

Huanlong Zheng received his B.S. degree from Northeast Forestry University in 2021. He is currently working toward the M.S. degree in Jilin University. His current researches focus on the synthesis of small molecule fluorescent probes and their applications.

Jianan Dai received his M.S. degree from Jilin University of China in 2019. He is currently working toward the PhD degree in the Electronics Science and Engineering Department, Jilin University. His current researches focus on the synthesis of small molecule fluorescent probes and their applications.

Huaiyu Li received his B.S. degree from Changchun University of Science and Technology in 2022. She is currently working toward the M.S. degree in the Electronics Science and Engineering Department, Jilin University. Her current researches focus on the organic fluorescent molecules for bio-imaging.

Ri Zhou received his PhD degree from Jilin University of China in 2021. He is now a postdoctoral fellow at Electronics Science and Engineering Department, Jilin University. His current researches focus on the synthesis of small molecule fluorescent probes and their applications.

Chenguang Wang received his PhD degree from the College of Chemistry, Jilin University in 2013. He then joined the Institute of Transformative Bio-Molecules, Nagoya University as a postdoctoral fellow. In 2019, he joined the College of Electronic Science and Engineering, Jilin University as a professor. His research interests focus on the design and synthesis of organic fluorescent molecules and their applications in fluorescence bio-imaging.

Yuan Gao received her PhD degree from Department of Analytical Chemistry at Jilin University in 2012. Now she is an professor in Jilin University, China. Her current research is focus on the preparation and application of graphene and semiconductor oxide, especial in gas sensor and biosensor.

Lijun Wang received the B. S. degree in electronic sciences in 1973 from Jilin University of China. Now he is a professor of Changchun Institute of Optics, Fine Mechanics and Physics, Chinese Academy of Sciences. His research interests focus on the laser technology and the relative optoelectronic application.

Peng Sun received his PhD degree from College of Electronic Science and Engineering, Jilin University, China in 2014. Now he is a professor of Jilin University. He is engaged in the gas sensors based on oxide semiconductors.

Fangmeng Liu received his PhD degree in 2017 from College of Electronic Science and Engineering, Jilin University, China. Now he is a professor of Jilin University, China. His current research interests include the application of functional materials and development of solid-state electrolyte gas sensor and flexible device.

Geyu Lu received the B. S. degree in electronic sciences in 1985 and the M. S. degree in 1988 from Jilin University of China and the Dr. Eng. degree in 1998 from Kyushu University of Japan. Now he is a professor of Jilin University, China. His current research interests include the development of chemical sensors and the application of the function materials.